ARTICLE

OBC
www.rsc.org/obc

An *ab-initio* study of some homolytic substitution reactions of acyl radicals at silicon, germanium and tin †

Hiroshi Matsubara *[a] and Carl H. Schiesser[b]

[a] *Department of Chemistry, Faculty of Arts and Sciences, Osaka Prefecture University, Sakai, Osaka 599-8531, Japan*

[b] *School of Chemistry, Bio21 Molecular Science and Biotechnology Institute, The University of Melbourne, Victoria 3010, Australia*

Received 18th August 2003, Accepted 7th October 2003
First published as an Advance Article on the web 29th October 2003

Ab initio calculations using the 6-311G**, cc-pVDZ, and (valence) double-ζ pseudopotential (DZP) basis sets, with (MP2, QCISD, CCSD(T)) and without (UHF) the inclusion of electron correlation, and density functional (BHandHLYP, B3LYP) calculations predict that homolytic substitution reactions of acetyl radicals at the silicon atoms in disilane can proceed *via* both backside and frontside attack mechanisms. At the highest level of theory (CCSD(T)/cc-pVDZ//MP2/cc-pVDZ), energy barriers ($\Delta E^{\ddagger}$) of 77.2 and 81.9 kJ mol^{-1} are calculated for the backside and frontside reactions respectively. Similar results are obtained for reactions involving germanium and tin with energy barriers ($\Delta E^{\ddagger}$) of 53.7–84.2, and 55.0–89.7 kJ mol^{-1} for the backside and frontside mechanisms, respectively. These data suggest that both homolytic substitution mechanisms are feasible for homolytic substitution reactions of acetyl radicals at silicon, germanium, and tin. BHandHLYP calculations provide geometries and energy barriers for backside and frontside transition states in good agreement with those obtained by traditional *ab initio* techniques.

Introduction

Homolytic substitution (S_H2) reactions are now widely used in organic synthesis and have been well documentated.[1,2] Despite this, reactions of this type at heteroatoms such as silicon, germanium and tin have not yet been fully explored.[3] In order to address these issues, work in our laboratories over the past few years has been directed toward the design, application and understanding of free-radical homolytic substitution chemistry with the aim of developing novel synthetic methodology.[4,5] To that end, we have published recently several *ab initio* studies with the aim of increasing our understanding of the factors that affect and control the mechanism of homolytic substitution at several main-group higher heteroatoms.[4–9] It is generally agreed that homolytic substitution reactions by an attacking radical (R) involve the approach of the radical at the heteroatom (Y) along a trajectory opposite to the leaving group (Z). This *backside* mechanism can proceed either *via* a transition state **1** in which the attacking and leaving radicals adopt a collinear (or near so) arrangement resulting in Walden inversion, or with the involvement of a hypervalent intermediate **2** which may or may not undergo pseudorotation prior to dissociation.[1,6]

In addition to the pathways for homolytic substitution described above, a mechanism involving *frontside* attack *via* transition state **3** has also recently been investigated. Calculations strongly suggest that the *frontside* attack pathway is involved in homolytic 1,2-translocation reactions between group (IV) elements,[7] while both *frontside* and *backside* mechanisms are predicted to have similar energy profiles for degenerate intermolecular homolytic substitution reactions involving silicon, germanium and tin.[8] In addition, recent studies on homolytic substitution reactions of a methyl radical at group (IV) heteroatoms also predict that the reaction can proceed *via* both of the above-mentioned mechanisms.

It has also been established that acyl radicals undergo homolytic substitution reactions at heteroatoms. For example, Ryu and co-workers reported that radical carbonylation followed by

1 **2** **3**

intramolecular substitution at sulfur affords γ-thiolactones.[10] Very recently, our coworkers discovered an intramolecular example of a homolytic substitution reaction involving an acyl radical; acyl radical **4** undergoes ring-closure at silicon with expulsion of stannyl radical to afford 1,1-diphenylsilacyclopentan-2-one (**5**) (Scheme 1).[11]

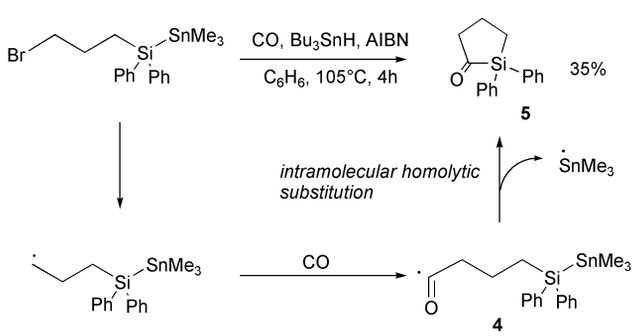

Scheme 1

Intrigued by this observation, and as part of our ongoing interest in homolytic substitution chemistry involving main group higher heteroatoms, we have investigated the homolytic substitution chemistry of acetyl radicals with disilane, digermane, distannane, silylgermane, silylstannane, and germylstannane by computational techniques.

Methods

Ab initio and DFT molecular orbital calculations were carried out on Compaq Personal Workstation 600au and Alpha Station DS10L computers using the Gaussian 98 program.[12] Geometry optimizations were performed using standard gradient techniques at the SCF, MP2, BHandHLYP and B3LYP

† Electronic supplementary information (ESI) available: optimized geometries and energies for all transition structures (Gaussian Archive entries). See http://www.rsc.org/suppdata/ob/b3/b309938e/

DOI: 10.1039/b309938e

Table 1 Calculated energy barriers[a] for the forward ($\Delta E_1^{\ddagger}$) and reverse ($\Delta E_2^{\ddagger}$) homolytic substitution reactions of acetyl radicals with disilane (Si_2H_6) and imaginary frequencies (ν)[b] of transition states **6** and **7**

	6					**7**				
Method	$\Delta E_1^{\ddagger}$	$\Delta E_1^{\ddagger}$+ZPE	$\Delta E_2^{\ddagger}$	$\Delta E_2^{\ddagger}$+ZPE	ν	$\Delta E_1^{\ddagger}$	$\Delta E_1^{\ddagger}$+ZPE	$\Delta E_2^{\ddagger}$	$\Delta E_2^{\ddagger}$+ZPE	ν
UHF/6-311G**	152.3	152.2	119.1	119.7	1734i	151.4	154.1	118.2	121.6	611i
UHF/DZP	151.9	151.9	122.1	123.1	1570i	154.3	157.0	124.6	128.2	606i
MP2/6-311G**	81.1	80.9	66.0	67.5	1225i	79.4	82.1	64.4	68.7	404i
MP2/DZP	84.5	85.0	64.3	66.9	1131i	86.4	89.4	66.2	71.3	423i
MP2/cc-pVDZ	82.9	82.9	61.2	62.6	1191i	81.8	84.2	60.1	63.9	404i
QCISD/6-311G**//MP2/6-311G**	85.9	—	60.7	—	—	90.3	—	65.1	—	—
QCISD/DZP//MP2/DZP	85.8	—	55.0	—	—	94.5	—	63.7	—	—
QCISD/cc-pVDZ//MP2/cc-pVDZ	85.7	—	54.5	—	—	92.1	—	60.9	—	—
CCSD(T)/6-311G**//MP2/6-311G**	76.7	—	53.8	—	—	79.6	—	56.7	—	—
CCSD(T)/DZP//MP2/DZP	77.7	—	49.6	—	—	84.6	—	56.5	—	—
CCSD(T)/cc-pVDZ//MP2/cc-pVDZ	77.2	—	48.1	—	—	81.9	—	52.8	—	—
BHandHLYP/6-311G**	83.4	84.1	50.9	52.6	707i	92.0	94.4	59.5	62.9	368i
BHandHLYP/DZP	82.7	83.4	55.3	57.4	695i	92.7	95.1	65.2	69.1	382i
B3LYP/6-311G**	58.5	59.3	27.3	29.2	360i	71.8	73.9	40.6	43.8	266i
B3LYP/DZP	58.0	58.9	31.8	34.2	379i	72.6	74.7	46.4	50.0	287i

[a] Energies in $kJmol^{-1}$. [b] Frequencies in cm^{-1}.

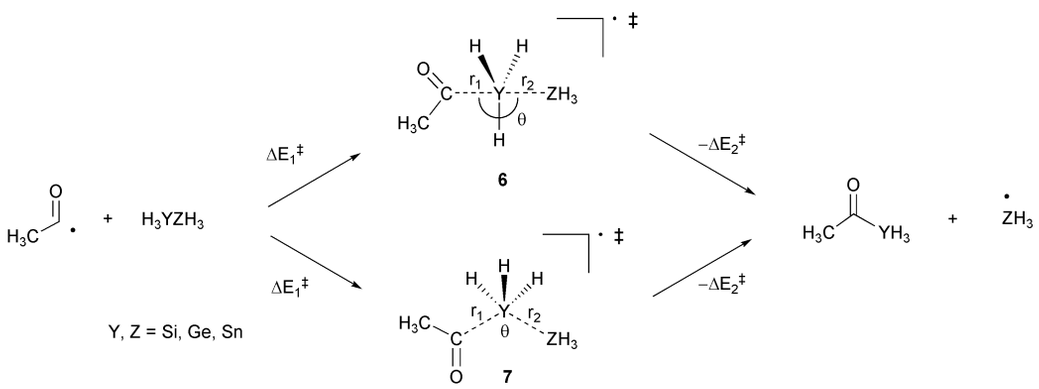

Scheme 2

levels of theory using restricted (RHF, RMP2, RBHandHLYP and RB3LYP) and unrestricted (UHF, UMP2, UBHandHLYP and UB3LYP) methods for closed- and open-shell systems respectively.[13] All ground and transition states were verified by vibrational frequency analysis. Further single-point QCISD and CCSD(T) calculations were performed on each of the MP2 optimized structures. When correlated methods were used, calculations were carried out using the frozen core approximation. Values of $<s^2>$ never exceeded 0.86 before annihilation of quartet contamination (except for some UHF calculations involving tin) and mostly differed from 0.75 by less than 10% at correlated levels of theory. Where appropriate, zero-point vibrational energy (ZPE) corrections have been applied. Standard basis sets were used, as well as the (valence) double-ζ pseudopotential basis sets of Hay and Wadt[14] supplemented with a single set of *d*-type polarization functions for the heteroatoms in this study, (exponents $d(\zeta)_{Si} = 0.284$,[15] $d(\zeta)_{Ge} = 0.230$,[15] and $d(\zeta)_{Sn} = 0.200$),[16] together with the double-ζ all-electron basis sets of Dunning and Hay[17] with an additional set of polarization functions (exponents $d(\zeta)_C = 0.75$ (Y = Z = Si), $d(\zeta)_O = 0.85$ and $p(\zeta)_H = 1.00$) for C, O and H. We refer to this basis set as DZP throughout this work.[5,7–9] In previous work, results generated using DZP proved to be very similar to those obtained using 6-311G** for reactions involving chlorine and silicon.[5,7–9]

Results and discussion

Homolytic substitution reactions of acetyl radical with disilane (Si_2H_6)

Extensive searching of the $H_3CCOSiH_3SiH_3$ (Scheme 2, Y = Z = Si) potential energy surfaces at the UHF/6-311G**, UHF/DZP, MP2/6-311G**, MP2/DZP, MP2/cc-pVDZ, BHandHLYP/6-311G**, BHandHLYP/DZP, B3LYP/6-311G**, and B3LYP/DZP levels of theory located hypervalent species **6** (Y = Z = Si) and **7** (Y = Z = Si) as transition states for the homolytic substitution of acetyl radicals at the silicon atom in disilane (Scheme 2). Both structures **6** and **7** proved to be of C_1 symmetry It is interesting to compare these results with those of our previous studies in which both *frontside* and *backside* transition states (**8**, **9**) were found to be involved when radicals such as methyl, silyl, germyl and stannyl are reacted with group(IV)-containing substrates.[8,9]

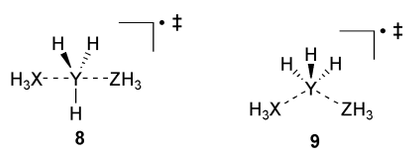

The important geometric features of the transition states **6** (Y = Z = Si) and **7** (Y= Z = Si) are summarized in Fig. 1, while calculated energy barriers ($\Delta E^{\ddagger}_1$ and $\Delta E^{\ddagger}_2$, Scheme 3) together with the corresponding transition state imaginary frequencies are listed in Table 1. Full computational details are available as ESI. †

Inspection of Fig. 1 reveals that while transition state **6** (Y = Z = Si) is predicted to adopt a near collinear arrangement (θ = 176–177°) of the attacking acetyl radical and the leaving silyl radical at all levels of theory employed, structure **7** (Y = Z = Si) involved in the analogous *frontside* chemistry is predicted to contain an attack angle (θ) of around 77° at all levels of theory; this angle is slightly smaller than those predicted for the *frontside* transition states involved in other homolytic substitution

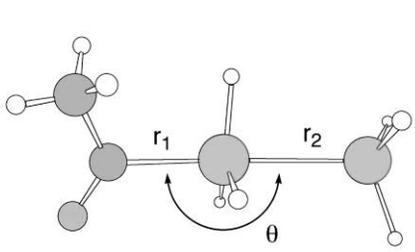

6

	r_1	r_2	θ
UHF/6-311G**	2.168 Å	2.592 Å	177.0°
UHF/DZP	2.167 Å	2.581 Å	177.3°
MP2/6-311G**	2.083 Å	2.562 Å	176.0°
MP2/DZP	2.088 Å	2.569 Å	176.9°
MP2/cc-pVDZ	2.109 Å	2.591 Å	176.7°
BHandHLYP/6-311G**	2.096 Å	2.559 Å	176.7°
BHandHLYP/DZP	2.102 Å	2.555 Å	177.0°
B3LYP/6-311G**	2.084 Å	2.630 Å	177.1°
B3LYP/DZP	2.092 Å	2.614 Å	177.1°

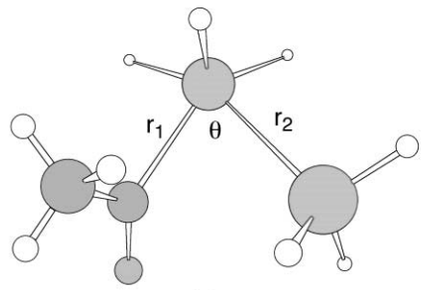

7

	r_1	r_2	θ
UHF/6-311G**	2.160 Å	2.598 Å	77.0°
UHF/DZP	2.152 Å	2.580 Å	77.0°
MP2/6-311G**	2.077 Å	2.537 Å	75.2°
MP2/DZP	2.089 Å	2.509 Å	75.9°
MP2/cc-pVDZ	2.116 Å	2.543 Å	75.7°
BHandHLYP/6-311G**	2.099 Å	2.529 Å	78.1°
BHandHLYP/DZP	2.093 Å	2.521 Å	77.9°
B3LYP/6-311G**	2.111 Å	2.534 Å	79.8°
B3LYP/DZP	2.100 Å	2.523 Å	79.5°

Fig. 1 Optimized structure of transition state **6** and **7** (Y = Z = Si) for the backside and frontside substitution reactions of acetyl radicals with disilane.

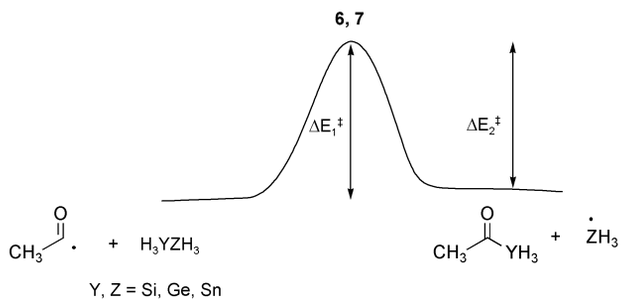

Scheme 3

reactions involving silyl, germyl and stannyl radicals.[8,9] The transition state (Si–Si) separations in **6** (Y = Z = Si) and **7** (Y = Z = Si) are predicted at all levels of theory to lie in the range: 2.555 Å–2.630 Å and 2.509 Å–2.598 Å, respectively, while the (C–Si) distances in **6** (Y = Z = Si) and **7** (Y = Z = Si) are calculated to be 2.083 Å–2.168 Å, and 2.077 Å–2.160 Å, respectively. The (Si–Si) separations are in the expected ranges when compared with our previous calculations,[8,9,18] while the (C–Si) distances are predicted to be slightly shorter than those of other homolytic substitution transition states, consistent with the expected orbital requirements of the resonance-stabilized acetyl radical.[19] Comparison with the reaction of methyl radical, the (C–Si) distances are shorter and the (Si–Si) separations are longer, indicating that the reaction of acetyl radical are predicted to have 'later' transition states than the methyl radical.

Not unexpectedly,[8,9] the data provided by this computational study suggests that the energy requirements for both homolytic pathways are similar. However, these reactions are predicted to be significantly endothermic at all levels of theory, with the reverse energy barrier being some 20–30 kJ mol^{-1} lower than the forward barrier in each case and at each level of theory. Inspection of Table 1 reveals that the energy barrier ($\Delta E_1^{\ddagger}$) for the forward reactions (Scheme 3) associated with **6** (Y = Z = Si) and **7** (Y = Z = Si) are calculated to be 152.3 and 151.4 kJ mol^{-1} respectively at the UHF/6-311G** level of theory. As expected, electron correlation is important in these calculations; MP2/6-311G** serves to lower these energy barriers to 81.1 and 79.4 kJ mol^{-1} for **6** (Y = Z = Si) and **7** (Y = Z = Si) respectively; however inclusion of zero-point vibrational energy correction (ZPE) has little effect on these barriers. Further improvements in both the basis set quality and levels of correlation provide values of $\Delta E_1^{\ddagger}$ for the reaction involving **6** (Y = Z = Si) that range from 82.9 (MP2/cc-pVDZ) to 85.9 (QCISD/6-311G**//MP2/6-311G**). In comparison, reactions involving **7** (Y = Z = Si) are calculated to have values of $\Delta E^{\ddagger}_1$ in the range: 81.8 to 90.3 kJ mol^{-1} at the same levels of theory. At the highest level of theory used (CCSD(T)/cc-pVDZ//MP2/cc-pVDZ), energy barriers ($\Delta E_1^{\ddagger}$) of 77.2 and 81.9 kJ mol^{-1} are predicted for the reaction involving **6** (Y = Z = Si) and **7** (Y = Z = Si), respectively. BHandHLYP/6-311G** calculation provides energy barriers ($\Delta E_1^{\ddagger}$) of 83.4 and 92.0 kJ mol^{-1} for the reaction involving **6** (Y = Z = Si) and **7** (Y = Z = Si) respectively, while values of 58.5 and 71.8 kJ mol^{-1} are obtained at the B3LYP/6-311G** level of theory. As the difference between the two pathways involving **6** (Y = Z = Si) and **7** (Y = Z = Si) is calculated to be only 4.7 kJ mol^{-1} at the highest level of theory, we conclude that homolytic substitution by an acetyl radical at disilane can proceed by either *backside* or *frontside* mechanisms. It should also be noted that the energy barriers for these reactions are calculated to be some 20 kJ mol^{-1} higher than those for the homolytic substitution of methyl radicals with disilane.[9] However, most importantly, the data suggest strongly that the reverse reaction, namely the attack by a silyl radical at the silicon atom in 1-silaacetone with expulsion of the acetyl radical is the preferred pathway, with both *frontside* and *backside* pathways feasible.

Homolytic substitution reaction of acetyl radicals with digermane (Ge_2H_6), distannane (Sn_2H_6), silylgermane (H_3SiGeH_3), silylstannane (H_3SiSnH_3), and germylstannane (H_3GeSnH_3)

Extensive searching of the $H_3CCOYH_3ZH_3$ (Y, Z = Si, Ge, Sn) potential energy surfaces at the UHF/DZP, MP2/DZP, BHandHLYP/DZP and B3LYP/DZP levels of theory located transition states **6** (Y, Z = Si, Ge, Sn) and **7** (Y, Z = Si, Ge, Sn). Interestingly, two *frontside* transition states with different symmetry are predicted to lie on the reaction pathway of the acetyl radical with distannane (Fig. 2). The important geometric features of these structures are summarised in Table 2 and the calculated energy barriers ($\Delta E_1^{\ddagger}$ and $\Delta E_2^{\ddagger}$ for the forward and reverse reactions respectively) are listed in Table 3. Full structural details and calculated energy barriers at all levels of theory employed in this study are found in the ESI (Tables S1 and S2)†.

Not surprisingly, transition states **6** (Y, Z = Si, Ge, Sn) and **7** (Y, Z = Si, Ge, Sn) bear a strong resemblance to those calculated for the analogous reactions with disilane **6** (Y = Z = Si)

Table 2 MP2/DZP, BHandHLYP/DZP, and B3LYP/DZP calculated important geometric features[a] of the transition states **6** and **7**

			6			**7** (C_1 symmetry)			**7** (C_s symmetry)		
Y	Z	Method	r_1	r_2	θ	r_1	r_2	θ	r_1	r_2	θ
Si	Ge	MP2/DZP	2.105	2.634	176.7	2.097	2.598	74.9	—	—	—[b]
		BHandHLYP/DZP	2.130	2.609	176.8	2.109	2.599	77.4	—	—	—[b]
		B3LYP/DZP	2.136	2.635	176.9	2.115	2.608	78.6	—	—	—[b]
Si	Sn	MP2/DZP	2.135	2.814	176.6	—	—	—[b]	2.134	2.772	78.4
		BHandHLYP/DZP	2.179	2.779	176.8	—	—	—[b]	2.141	2.785	78.5
		B3LYP/DZP	2.217	2.777	176.8	—	—	—[b]	2.122	2.835	79.3
Ge	Si	MP2/DZP	2.185	2.679	177.5	2.190	2.606	74.2	—	—	—[b]
		BHandHLYP/DZP	2.195	2.674	177.8	2.199	2.626	76.3	—	—	—[b]
		B3LYP/DZP	2.190	2.735	178.0	2.211	2.624	78.1	—	—	—[b]
Ge	Ge	MP2/DZP	2.199	2.741	177.3	2.196	2.695	73.1	—	—	—[b]
		BHandHLYP/DZP	2.217	2.726	177.6	2.218	2.700	75.9	—	—	—[b]
		B3LYP/DZP	2.221	2.762	177.7	2.228	2.706	77.3	—	—	—[b]
Ge	Sn	MP2/DZP	2.223	2.912	177.2	—	—	—[b]	2.222	2.878	76.0
		BHandHLYP/DZP	2.255	2.894	177.6	—	—	—[b]	2.228	2.916	75.7
		B3LYP/DZP	2.275	2.906	177.5	—	—	—[b]	2.229	2.953	77.0
Sn	Si	MP2/DZP	2.361	2.855	179.4	2.351	2.828	69.9	—	—	—[b]
		BHandHLYP/DZP	2.347	2.871	177.5	2.346	2.868	72.3	—	—	—[b]
		B3LYP/DZP	2.332	2.970	178.9	2.327	2.917	74.4	—	—	—[b]
Sn	Ge	MP2/DZP	2.370	2.919	179.4	2.367	2.886	70.1	—	—	—[b]
		BHandHLYP/DZP	2.361	2.924	177.4	2.380	2.904	72.6	—	—	—[b]
		B3LYP/DZP	—	—	—[b]	2.374	2.917	75.0	—	—	—[b]
Sn	Sn	MP2/DZP	2.382	3.096	179.7	2.380	3.067	69.6	2.392	3.078	72.0
		BHandHLYP/DZP	2.384	3.089	177.4	2.409	3.067	72.6	2.393	3.119	72.0
		B3LYP/DZP	2.383	3.129	177.6	2.420	3.069	74.5	2.406	3.127	74.4

[a] Distance in Å and angles in deg. [b] No transition states were found.

Table 3 Calculated energy barriers[a] on the CCSD(T)/DZP//MP2/DZP level of theory for the forward ($\Delta E_1^{\ddagger}$) and reverse ($\Delta E_2^{\ddagger}$) homolytic substitution reactions of acetyl radical with digermane (Ge_2H_6), distannane (Sn_2H_6), silylgermane (H_3SiGeH_3), silylstannane (H_3SiSnH_3), and germylstannane (H_3GeSnH_3) of transition states **6** and **7**

		6		**7** (C_1 symmetry)		**7** (C_s symmetry)	
Y	Z	$\Delta E_1^{\ddagger}$	$\Delta E_2^{\ddagger}$	$\Delta E_1^{\ddagger}$	$\Delta E_2^{\ddagger}$	$\Delta E_1^{\ddagger}$	$\Delta E_2^{\ddagger}$
Si	Ge	65.1	59.1	74.9	68.9	—	—[b]
Si	Sn	53.7	75.5	—	—[b]	60.3	82.1
Ge	Si	84.2	46.5	89.7	52.0	—	—[b]
Ge	Ge	72.3	54.0	80.3	62.1	—	—[b]
Ge	Sn	61.5	66.7	—	—[b]	66.4	71.6
Sn	Si	79.7	31.9	71.8	24.0	—	—[b]
Sn	Ge	70.6	37.9	63.6	31.0	—	—[b]
Sn	Sn	60.8	47.0	57.0	43.2	55.0	41.2

[a] Energies in kJ mol^{-1}. [b] No transition states were found.

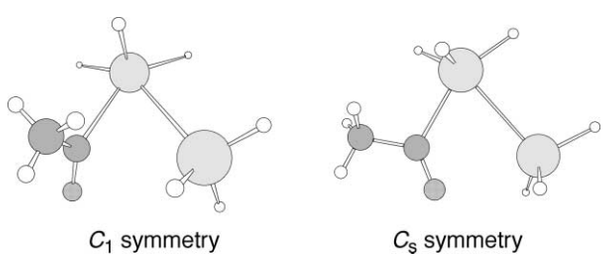

Fig. 2 Structures of the frontiside transition state **7** (Y = Z = Sn).

and **7** (Y = Z = Si). *Backside* attack structures **6** (Y = Z = Si, Ge, Sn) are predicted to adopt a near collinear arrangement of attacking and leaving radicals, while the *frontside* structures **7** (Y, Z = Si, Ge; Y = Sn, Z = Si, Ge, Sn) of C_1 symmetry are calculated to have angles (θ) of about 70–80° between attacking and leaving species. Interestingly, the frontside transition states **7** involving tin as the leaving radical (Y = Si, Ge, Sn; Z = Sn), are predicted to adopt C_s symmetry with similar attacking angles to those predicted for the analogous C_1 isomers.

As can be seen in Table 2, C–Y distances (r_1) in **6** are calculated to lie between 2.105 (Y = Si, Z = Ge) and 2.382 Å (Y = Z = Sn) at the MP2/DZP level of theory, while Y–Z separations (r_2) in **6** are predicted to be in the range: 2.634 (Y = Si, Z = Ge)–3.096 Å (Y = Z = Sn). Similar trends are also observed for **7**, the transition stated involved in the *frontside* mechanism at the MP2/DZP level of theory. Interestingly, it should be noted that B3LYP calculations predict structures for **6** and **7** with larger angles and greater separations than those calculated using more traditional methods, while the BHandHLYP method provides geometries close to those obtained with the MP2/DZP level of theory.

Inspection of Table 3 and S2† reveals that some interesting trends in energy are clearly evident. As can be seen in the Tables, most of calculated energy barriers ($\Delta E_2^{\ddagger}$) for the reverse reactions (Scheme 3) are smaller than those ($\Delta E_1^{\ddagger}$) for the forward processes, indicating these reactions are predicted to be endothermic. However, in the cases of (Y = Si, Ge and Z = Sn) the reactions involving both transition states are calculated to be exothermic at all levels of theory. Once again, the calculated energy barriers ($\Delta E^{\ddagger}$) are also affected strongly by the inclusion of electron correlation. Interestingly, $\Delta E^{\ddagger}$ for both isomers of the *frontside* transition states **7** (Y = Z = Sn) are calculated to be very similar; however, the energy barrier for the transition state with C_s symmetry is predicted to slightly smaller than that with C_1 symmetry. At any given level of theory, the values of $\Delta E_1^{\ddagger}$

Table 4 BHandHLYP/DZP calculated important geometric features[a] of the transition states **10** and **11**

		10			**11** (C_1 symmetry)			**11** (C_s symmetry)		
Y	Z	r_1	r_2	θ	r_1	r_2	θ	r_1	r_2	θ
Si	Si	2.137	2.499	176.9	2.079	2.523	80.9	—	—	—[b]
Si	Ge	2.160	2.564	176.9	2.079	2.614	79.0	—	—	—[b]
Si	Sn	2.200	2.747	176.7	—	—	—[b]	2.143	2.765	81.4
Ge	Si	2.215	2.614	177.8	2.181	2.628	79.9	—	—	—[b]
Ge	Ge	2.235	2.679	177.7	2.192	2.705	78.4	—	—	—[b]
Ge	Sn	2.265	2.858	177.5	—	—	—[b]	2.214	2.905	78.0
Sn	Si	2.371	2.804	177.8	2.368	2.821	76.4	—	—	—[b]
Sn	Ge	2.382	2.868	177.8	2.383	2.897	74.4	—	—	—[b]
Sn	Sn	2.396	3.045	177.7	—	—	—[b]	2.379	3.105	74.6

[a] Distances in Å and angles in deg. [b] No transition states were found.

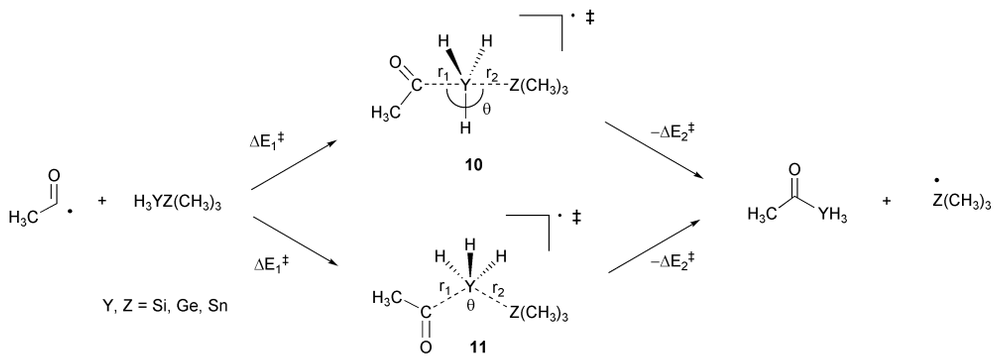

Scheme 4

and $\Delta E_2^{\ddagger}$ are clearly dependent on the nature of the atom undergoing homolytic substitution and the nature of the leaving radical. As observed in previous work, for given attacking and leaving radicals involved in attack at group(IV) heteroatoms, the order of reactivity is usually: Sn > Si ≥ Ge.[8] It is noteworthy that the results obtained in this work for chemistry involving *frontside* transition states reveal the same trend, namely that the order of reactivity of the *frontside* mechanism for the attack of an acetyl radical at a group(IV) heteroatom with the same leaving group is: Sn > Si > Ge, while the order of reactivity for reactions involving the *backside* mechanism is: Si > Sn > Ge. For example, at the highest level of theory (CCSD(T)/DZP//MP2/DZP) values of 89.7 and 71.8 kJ mol^{-1} are calculated for the *frontside* attack of acetyl radical at the germanium and tin atom in silylgermane and silylstannane (silyl radical as a leaving group), respectively. These numbers are to be compared with the value of 84.6 kJ mol^{-1} (Table 1) for the analogous reaction with disilane at the same level of theory. On the other hand, the energy barriers for analogous reactions involving *backside* transition state **6** are predicted 77.7 (Si), 84.2 (Ge), and 79.7 kJ mol^{-1} (Sn) at the highest level of theory.

Importantly, the computational data presented in this work indicate that both *frontside* and *backside* attack mechanisms are predicted to be feasible at all levels of theory employed. For example, at CCSD(T)/DZP//MP2/DZP level of theory, the *backside* reaction is favoured over the reaction involving **7** by 6.6–9.8 kJ mol^{-1} for attack at silicon and by 4.9–8.0 kJ mol^{-1} for attack at germanium. However, the *frontside* mechanism is predicted to be favoured slightly for reactions involving attack at tin at all levels of theory (except B3LYP/ZDP); CCSD(T)/DZP//MP2/DZP calculations predict that the *frontside* process involving tin is favoured by 7.9 kJ mol^{-1} (Z = Si), 7.0 kJ mol^{-1} (Z = Ge) and 3.8 kJ mol^{-1} (Z = Sn).

Effect of alkyl substitution – homolytic substitution reaction of acetyl radical with H_3YZMe_3. (Y, Z = Si, Ge, Sn)

As described above, apart from a few exceptions, the majority of reactions described so far have been endothermic, in other words, acetyl radicals prefer to be the leaving group rather than the attacking species. In order to explore the factors that affect this chemistry further, we briefly examined the effect of alkyl substitution on the reactions in question. Accordingly, the reactions of acetyl radicals with species H_3YZMe_3, in which the trimethylsilyl, trimethylgermyl and trimethylstannyl moieties were chosen as leaving groups were modeled. Because of significant increases in computational size, and given that the BHandHLYP method performed well in the above-mentioned work, the reaction profiles described in Scheme 4 were examined using this method. Thus, extensive searching of the $H_3CCOYH_3ZC_3H_9$ (Y, Z = Si, Ge, Sn) potential energy surfaces at the BHandHLYP/DZP level of theory located transition states **10** (Y, Z = Si, Ge, Sn) and **11** (Y, Z = Si, Ge, Sn). The important geometric features of these structures are summarised Table 4, and the calculated energy barriers are listed in Table 5. Full structural details are available as ESI †.

Not unexpectedly, transition states **10** and **11** are calculated to have similar structures to **6** and **7**. *Backside* attack structures **10** are predicted to adopt a near collinear arrangement of attacking and leaving radicals, while the *frontside* transition states **11** with a trimethylstannyl group as the leaving radical are predicted to have C_s symmetry; the *frontside* structure with other combinations of group (IV) atoms are calculated to have C_1 symmetry. Attacking angles (θ) are calculated to be about 74–82°, which are slightly larger than those in the transition states **7**.

As can be seen in Table 4, (C–Y) distances (r_1) in **10** and **11** are calculated to be longer than those in **6** and **7**, while (Y–Z) separations (r_2) in **10** and **11** are predicted to be shorter than those in **6** and **7**, indicating that the trimethyl substituted transition states **10** and **11** are calculated to be 'earlier' than transition states **6** and **7**.

Inspection of Table 5 reveals that most of the reactions in question are still predicted to be endothermic, despite alkyl substitution on the leaving radical. Importantly, the one exception to this trend involves the reaction of trimethylstannylsilane ($H_3SiSnMe_3$) which is predicted to be exothermic by about

Table 5 Calculated energy barriers[a] on the BHandHLYP/DZP level of theory for the forward ($\Delta E_1^{\ddagger}$) and reverse ($\Delta E_2^{\ddagger}$) homolytic substitution reactions of acetyl radicals at silicon, germanium and tin with expulsion of trimethylsilyl, trimethylgermyl and trimethylstannyl radicals and imaginary frequencies (ν)[b] of transition states **10** and **11**

		10					**11**				
Y	Z	$\Delta E_1^{\ddagger}$	$\Delta E_1^{\ddagger}$+ZPE	$\Delta E_2^{\ddagger}$	$\Delta E_2^{\ddagger}$+ZPE	ν	$\Delta E_1^{\ddagger}$	$\Delta E_1^{\ddagger}$+ZPE	$\Delta E_2^{\ddagger}$	$\Delta E_2^{\ddagger}$+ZPE	ν
Si	Si	79.4	80.2	49.6	47.1	706i	82.8	86.4	53.0	53.3	349i
Si	Ge	70.9	72.0	60.4	57.6	697i	74.2	78.4	63.7	63.9	299i
Si	Sn	62.7	64.4	76.5	73.1	677i	61.5	65.2	75.2	73.9	286i
Ge	Si	89.5	90.0	47.3	44.8	616i	92.0	94.5	49.9	49.3	331i
Ge	Ge	80.5	81.3	55.5	52.5	613i	83.7	86.6	58.7	57.8	313i
Ge	Sn	72.2	73.4	67.1	63.7	611i	70.3	73.4	65.2	63.8	215i
Sn	Si	80.2	80.0	30.2	28.1	634i	71.4	73.5	21.5	21.7	268i
Sn	Ge	74.0	74.0	36.3	33.7	624i	66.6	69.3	29.0	29.0	257i
Sn	Sn	68.2	68.4	44.2	41.3	618i	58.2	60.8	34.3	33.7	202i

[a] Energies in kJ mol^{-1}. [b] Frequencies in cm^{-1}.

14 kJ mol^{-1}, irrespective of reaction mechanism (*frontside* or *backside*). It is perhaps not surprising then that the only reported experimental example of an acyl radical undergoing the type of homolytic chemistry described herein is that depicted in Scheme 1 and involves attack at silicon with expulsion of trimethylstannyl. The calculated energy barriers ($\Delta E_1^{\ddagger}$) for the reactions depicted in Scheme 4 are are slightly smaller than those for the corresponding unsubstituted molecules. Again, both *frontside* and *backside* attack mechanisms are predicted to be feasible. Interestingly, the *frontside* mechanism is predicted to be favoured slightly for reactions with tin as the leaving radical as well as ones involving attack at tin.

Conclusions

In conclusion, reactions of acetyl radicals with group(IV) heteroatom-containing systems in this study are predicted to be associated with high energy barriers and to be endothermic in all cases except for one example involving a stannylsilane. The calculated energy barriers suggest that in most cases these transformations are unlikely to be synthetically useful, however, homolytic substitutions of acyl radicals with stannylsilanes have synthetic possibilities that may provide entry into novel silylketone derivatives.

Acknowledgements

The support of the Melbourne Advanced Research Computing Centre is gratefully acknowledged.

References

1 For leading reviews, see: J. C. Walton, *Acc. Chem. Res.*, 1998, **31**, 99; C. H. Schiesser and L. M. Wild, *Tetrahedron*, 1996, **52**, 13265; J.-M. Saveant, *Tetrahedron*, 1994, **50**, 10117; A. L. J. Beckwith, *Chem. Soc. Rev.*, 1993, **22**, 143; R. A. Rossi and S. M. Palacios, *Tetrahedron*, 1993, **49**, 4485.

2 For some recent reports, see: P. Lightfoot, P. Pareschi and J. C. Walton, *J. Chem. Soc., Perkin Trans. 2*, 2002, 918; C. A. G. Carter, G. Greidanus, J.-X. Chen and J. M. Stryker, *J. Am. Chem. Soc.*, 2001, **123**, 8872; A. M. Stolzenberg and Y. Cao, *J. Am. Chem. Soc.*, 2001, **123**, 9078; S. E. Tichy, K. K. Thoen, J. M. Price, J. J. Ferra, Jr., C. J. Petucci and H. I. Kenttaemaa, *J. Org. Chem.*, 2001, **66**, 2726; N. Al-Maharik, L. Engman, J. Malmström and C. H. Schiesser, *J. Org. Chem.*, 2001, **66**, 6286; S.-K. Kang, H.-W. Seo and Y.-H. Ha, *Synthesis*, 2001, 1321; M.-J. Bourgeois, M. Vialemaringe, M. Campagnole and E. Mountaudon, *Can. J. Chem.*, 2001, **79**, 257; M. W. Carland, L. R. Martin and C. H. Schiesser, *Tetrahedron Lett.*, 2001, **42**, 4737; J. B. Miller and J. R. Salvador, *J. Org. Chem.*, 2002, **67**, 435; L. Benati, R. Leardini, M. Minozzi, D. Nanni, P. Spagnolo, S. Strazzari and G. Zanardi, *Org. Lett.*, 2002, **4**, 3079; J. Hartung, T. Gottwald and K. Spehar, *Synthesis*, 2002, 1469.

3 For some recent reports, see: A. Studer, *Angew. Chem., Int. Ed.*, 1998, **37**, 462; A. Studer and H. Steen, *Chem. Eur. J.*, 1999, **5**, 759; S. Amrein, M. Bossart, T. Vasella and A. Studer, *J. Org. Chem.*, 2000, **65**, 4281; A. Studer, M. Bossart and T. Vasella, *Org. Lett.*, 2000, **2**, 985.

4 C. H. Schiesser and B. A. Smart, *Tetrahedron*, 1995, **51**, 6051; C. H. Schiesser, B. A. Smart and T.-A. Tran, *Tetrahedron*, 1995, **51**, 10651; C. H. Schiesser and B. A. Smart, *J. Comput. Chem.*, 1995, **16**, 1055; M. C. Fong and C. H. Schiesser, *Tetrahedron Lett.*, 1995, **36**, 7329; C. H. Schiesser and M. A. Skidmore, *Chem. Commun.*, 1996, 1419; M. A. Lucas and C. H. Schiesser, *J. Org. Chem.*, 1996, **61**, 5754; M. C. Fong and C. H. Schiesser, *J. Org. Chem.*, 1997, **62**, 3103; M. J. Laws and C. H. Schiesser, *Tetrahedron Lett.*, 1997, **38**, 8429; M. A. Lucas and C. H. Schiesser, *J. Org. Chem.*, 1998, **63**, 3032; C. H. Schiesser and M. A. Skidmore, *J. Organomet. Chem.*, 1998, **552**, 145; C. H. Schiesser and L. M. Wild, *J. Org. Chem.*, 1999, **64**, 1131; L. Engman, M. J. Laws, J. Malmström, C. H. Schiesser and L. M. Zugaro, *J. Org. Chem.*, 1999, **64**, 6764; M. A. Lucas, O. T. K. Nguyen, C. H. Schiesser and S.-L. Zheng, *Tetrahedron*, 2000, **56**, 3995; S. Kim, S. M. Hovat and C. H. Schiesser, *Aust. J. Chem.*, 2002, **55**, 753; S. M. Hovat, S. Kim and C. H. Schiesser, *Chem. Commun.*, 2003, 1182.

5 C. H. Schiesser, B. A. Smart and T.-A. Tran, *Tetrahedron*, 1995, **51**, 3327; C. H. Schiesser and L. M. Wild, *J. Org. Chem.*, 1998, **63**, 670; C. H. Schiesser, M. L. Styles and L. M. Wild, *J. Chem. Soc., Perkin Trans. 2*, 1996, 2257.

6 C. H. Schiesser and L. M. Wild, *Aust. J. Chem.*, 1995, **48**, 175. See also: J. M. Howell and J. F. Olsen, *J. Am. Chem. Soc.*, 1976, **98**, 7119; C. J. Cramer, *J. Am. Chem. Soc.*, 1990, **112**, 7965; C. J. Cramer, *J. Am. Chem. Soc.*, 1991, **113**, 2439.

7 S. M. Horvat and C. H. Schiesser, *J. Chem. Soc., Perkin Trans. 2*, 2001, 939.

8 S. M. Horvat, C. H. Schiesser and L. M. Wild, *Organometallics*, 2000, **19**, 1239.

9 H. Matsubara, S. M. Horvat and C. H. Schiesser, *Org. Biomol. Chem.*, 2003, **1**, 1190.

10 I. Ryu, T. Okada, K. Nagahara, N. Kambe, M. Komatsu and N. Sonoda, *J. Org. Chem.*, 1997, **62**, 7550.

11 A. Studer, S. Amrein, H. Matsubara, C. H. Schiesser, T. Doi, T. Kawamura, T. Fukuyama and I. Ryu, *Chem. Commun.*, 2003, 1190.

12 M. J. Frisch, G. W. Trucks, H. B. Schlegel, G. E. Scuseria, M. A. Robb, J. R. Cheeseman, V. G. Zakrzewski, J. A. Montgomery, Jr., R. E. Stratmann, J. C. Burant, S. Dapprich, J. M. Millam, A. D. Daniels, K. N. Kudin, M. C. Strain, O. Farkas, J. Tomasi, V. Barone, M. Cossi, R. Cammi, B. Mennucci, C. Pomelli, C. Adamo, S. Clifford, J. Ochterski, G. A. Petersson, P. Y. Ayala, Q. Cui, K. Morokuma, D. K. Malick, A. D. Rabuck, K. Raghavachari, J. B. Foresman, J. Cioslowski, J. V. Ortiz, A. G. Baboul, B. B. Stefanov, G. Liu, A. Liashenko, P. Piskorz, I. Komaromi, R. Gomperts, R. L. Martin, D. J. Fox, T. Keith, M. A. Al-Laham, C. Y. Peng, A. Nanayakkara, C. Gonzalez, M. Challacombe, P. M. W. Gill, B. Johnson, W. Chen, M. W. Wong, J. L. Andres, C. Gonzalez, M. Head-Gordon, E. S. Replogle, and J. A. Pople, Gaussian 98, Revision A.7, Gaussian, Inc., Pittsburgh PA, 1998.

13 W. J. Hehre, L. Radom, P. v. R. Schleyer, and P. A. Pople, *Ab Initio Molecular Orbital Theory*, Wiley, New York, 1986.

14 W. R. Wadt and P. J. Hay, *J. Chem. Phys.*, 1985, **82**, 284; P. J. Hay and W. R. Wadt, *J. Chem. Phys.*, 1985, **82**, 270; P. J. Hay and W. R. Wadt, *J. Chem. Phys.*, 1985, **82**, 299.
15 A. Höllwarth, M. Böhme, S. Dapprich, A. W. Ehlers, A. Gobbi, V. Jonas, K. F. Köhler, R. Stegmann, A. Veldkamp and G. Frenking, *Chem. Phys. Lett.*, 1993, **208**, 237.
16 B. A. Smart, *PhD Thesis*, The University of Melbourne, 1994.
17 T. H. Dunning and P. J. Hay, *Modern Theoretical Chemistry*, Plenum, New York, 1976, ch. 1, pp. 1–28.
18 C. H. Schiesser and M. L. Styles, *J. Chem. Soc., Perkin Trans. 2*, 1997, 2335.
19 T. Morihovitis, C. H. Schiesser and M. A. Skidmore, *J. Chem. Soc., Perkin Trans. 2*, 1999, 2041; C. T. Falzon, I. Ryu and C. H. Schiesser, *Chem. Commun.*, 2002, 2338.